Molecular Therapy
Nucleic Acids
Original Article

# Allele-specific targeting of mutant ataxin-3 by antisense oligonucleotides in SCA3-iPSC-derived neurons

Stefan Hauser,[1,2] Jacob Helm,[1,2,3] Melanie Kraft,[1,2] Milena Korneck,[1,2,3] Jeannette Hübener-Schmid,[4] and Ludger Schöls[1,2]

[1]German Center for Neurodegenerative Diseases (DZNE), 72076 Tübingen, Germany; [2]Hertie Institute for Clinical Brain Research, University of Tübingen, 72076 Tübingen, Germany; [3]Graduate School of Cellular and Molecular Neuroscience, University of Tübingen, 72076 Tübingen, Germany; [4]Institute of Medical Genetics and Applied Genomics and Center of Rare Diseases, University of Tübingen, 72076 Tübingen, Germany

**Spinocerebellar ataxia type 3 (SCA3) is caused by an expanded polyglutamine stretch in ataxin-3. While wild-type ataxin-3 has important functions, e.g., as a deubiquitinase, downregulation of mutant ataxin-3 is likely to slow down the course of this fatal disease. We established a screening platform with human neurons of patients and controls derived from induced pluripotent stem cells to test antisense oligonucleotides (ASOs) for their effects on ataxin-3 expression. We identified an ASO that suppressed mutant and wild-type ataxin-3 levels by >90% after a singular treatment. Next, we screened pairs of ASOs designed to selectively target the mutant or the wild-type allele by taking advantage of a SNP (c.987G > C) in *ATXN3* that is present in most SCA3 patients. We found ASOmut4 to reduce levels of mutant ataxin-3 by 80% after 10 days while leaving expression of wild-type ataxin-3 largely unaffected. In a long-term study we proved this effect to last for about 4 weeks after a single treatment without signs of neurotoxicity. This study provides proof of principle that allele-specific lowering of poly(Q)-expanded ataxin-3 by selective ASOs is feasible and long lasting, with sparing of wild-type ataxin-3 expression in a human cell culture model that is genetically identical to SCA3 patients.**

## INTRODUCTION

Spinocerebellar ataxia type 3 (SCA3), also known as Machado-Joseph disease (MJD), is an autosomal dominantly inherited neurodegenerative disease caused by a cytosine-adenine-guanine (CAG) trinucleotide repeat expansion in the *ataxin-3* (*ATXN3*) gene.[1] The CAG repeat is translated into a prolonged polyglutamine stretch (poly(Q)) that is supposed to drive the pathogenic process via an abnormal gain of function (reviewed in Matos et al.[2]). Although the genetic cause of the disease is well characterized, the underlying pathomechanism leading to a selective neurodegeneration is still not fully clarified. Pathogenic mechanisms include the widespread formation of putative toxic ataxin-3 species (fragments, aggregates, neuronal nuclear inclusions [NNIs]), including brain stem, cerebellum, basal ganglia, and cortical regions,[3–7] as well as impairment of several cellular mechanisms like the ubiquitin-proteasome system,[8,9] autophagy,[10,11] calcium signaling,[12] transcriptional regulation,[13,14] and mitochondrial function.[15,16] Despite this extensive knowledge on the (dys)function of poly(Q)-expanded ataxin-3, no causative treatment to slow or stop the progression of the disease has been established.

Due to the multiple involved disease mechanisms, an ideal therapeutic strategy should focus on the silencing of the expanded CAG repeat, thereby positively influencing all downstream pathomechanisms. Therefore, several *in vitro* as well as *in vivo* studies aiming to reduce mutant *ATXN3* levels have been performed, including treatment with small interfering RNAs (siRNAs), short hairpin RNAs (shRNAs), microRNAs, and antisense oligonucleotides (ASOs) in cell models and transgenic rodents.[17–29] Results of these studies clearly demonstrated a functional benefit in lowering the expression of the pathogenic poly(Q)-expanded ataxin-3. As ataxin-3 has several important physiological functions and is involved in the proteasomal degradation pathway as a deubiquitinase, it appears desirable to develop a gene-silencing approach that selectively reduces poly(Q)-expanded ataxin-3 while preserving the wild-type protein as much as possible. This could be achieved by developing sequences targeting allele-specific intragenic single-nucleotide polymorphisms (SNPs). In SCA3, the SNP c.987G > C (rs12895357) at the 3′ end of the CAG repeat of *ATXN3*, which has been identified at a high frequency in SCA3 patients and is associated with the CAG-expanded *ATXN3* allele, might be a suitable target to achieve allele specificity.[30,31]

With the discovery of induced pluripotent stem cells (iPSCs), which can be generated from the somatic cells of patients, a promising *in vitro* model system to generate disease-relevant patient cells became available.[32] This model system enables us to study the effects of mutant ataxin-3 in human neuronal cell types with the patient's genetic background and an endogenous expression of *ATXN3*.[33–37]

Received 23 June 2021; accepted 16 November 2021;
https://doi.org/10.1016/j.omtn.2021.11.015.

**Correspondence:** Ludger Schöls, MD, German Center for Neurodegenerative Diseases (DZNE), 72076 Tübingen, Germany.
**E-mail:** ludger.schoels@uni-tuebingen.de

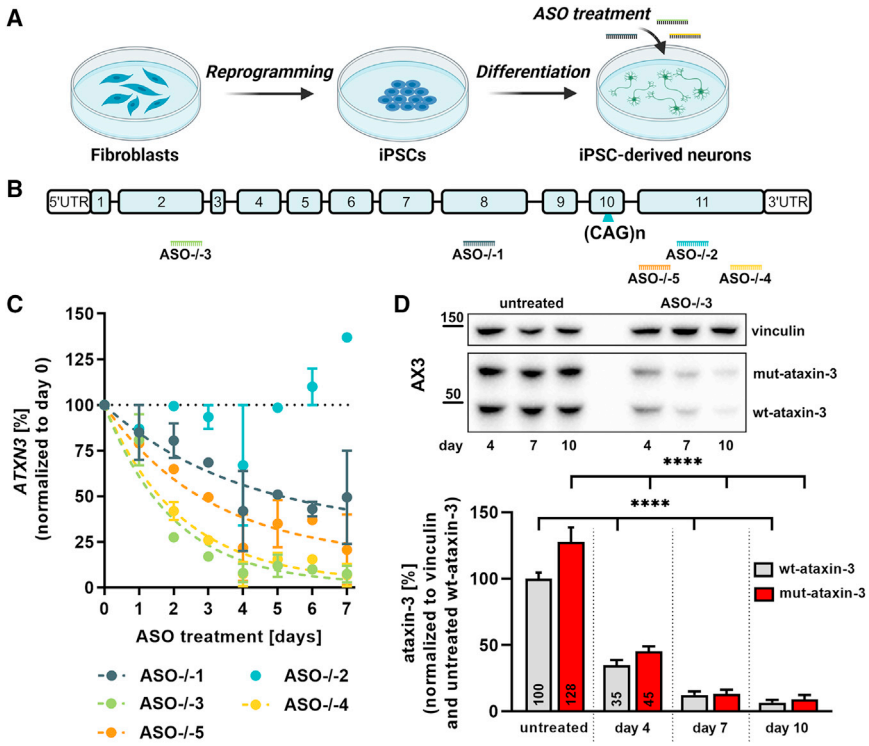


**Figure 1. Establishment of an iPSC-based *in vitro* model to screen ASOs for SCA3**

(A) Schematic representation of the experimental procedure to reprogram fibroblasts to iPSCs and differentiate them to iPSC-derived neurons for ASO treatments. (B) Scheme of the *ATXN3* gene structure and target sites of five non-selective ASOs (ASO−/−1 to ASO−/−5). (C) Transcript levels of *ATXN3* over 7 days of ASO−/−1 to ASO−/−5 treatment. Levels are normalized to untreated day 0. Data are presented as RQ ± $RQ_{min/max}$, n = 3. (D) ATXN3 protein expression of untreated and ASO−/−3-treated iPSC-derived neurons of patient AX3 analyzed by western blotting. Bands were quantified densitometrically and normalized to vinculin and untreated WT ataxin-3 levels. One representative blot is shown. Data are the mean ± SEM, n = 3, unpaired multiple t test (untreated to ASO treated), ****p < 0.0001.

In the present study we used iPSC-derived neurons generated from healthy controls and SCA3 patients to identify an optimal ASO that selectively and specifically reduces mutant ataxin-3 in a disease-relevant cell type. We established a neuronal cell model that is suitable as a screening tool and allows us to prove the efficacy and allele specificity of ASOs within 4 days of treatment. We were able to identify several ASOs that either specifically reduce mutant or wild-type ataxin-3 by targeting the SNP c.987G > C or lead to a stable and robust knockdown of total ataxin-3 without any obvious signs of neurotoxicity. Our study highlights disease-specific iPSC-derived neurons as an *in vitro* tool that endogenously expresses both *ATXN3* alleles to screen (allele-specific) ASOs to decrease the expression of mutant protein as a potential treatment for neurodegenerative diseases.

## RESULTS

### Establishing an iPSC-based platform to analyze the efficiency of ASOs at reducing ataxin-3

As SCA3 exclusively affects the peripheral and central nervous system, we established iPSC-derived neurons as an *in vitro* screening tool to analyze ASOs for their efficiency at reducing ataxin-3 levels. For this, we generated iPSCs from three SCA3 patients (AX1, AX2, and AX3) and three healthy controls (CO1, CO2, and CO3). All lines were intensively genomically and functionally characterized (for details see Hayer et al.[33]). In the next step, iPSCs were differentiated into iPSC-derived cortical neurons according to our previously published protocol.[38,39] After 36 days of differentiation, iPSC-derived neurons were then treated with ASOs targeting *ATXN3* (Figure 1A).

To establish optimum conditions for a potential ASO screening platform in iPSC-derived neurons, five different ASOs targeting both alleles of *ATXN3* (ASO−/−1 to ASO−/−5; Antisense LNA GapmeRs, Qiagen) were designed (Figure 1B). The potential of these ASOs to downregulate the expression of *ATXN3* was investigated via qRT-PCR. For this, iPSC-derived neurons were treated with the various ASOs (5 μM) for up to 7 days. RNA was isolated daily between 1 and 7 days. Treatment with the five ASOs showed a high variability in knockdown efficiency of *ATXN3* on mRNA level (Figure 1C). While treatment with ASO−/−2 did not result in a reduction of *ATXN3* expression, treatment with ASO−/−1 and ASO−/−5 led to a moderate knockdown and ASO−/−3 and ASO−/−4 to a strong and progressive reduction of *ATXN3* over time (>90% reduction after 7 days of treatment). Based on these results, ASO−/−3 was selected for further analysis of ataxin-3 protein level. For this, the SCA3 patient iPSC line (AX3) was differentiated into iPSC-derived neurons and treated with ASO−/−3 for 4, 7, or 10 days. Western blot analysis of untreated iPSC-derived neurons showed a stable expression of wild-type ataxin-3 (WT ataxin-3) and mutant poly(Q)-expanded ataxin-3 (mut-ataxin-3) over time. Treatment of neurons with ASO−/−3 resulted in a massive reduction of both WT and mut-ataxin-3 already after 4 days of treatment (~60% reduction), with an even more drastic effect after 7 (>80%) and 10 days of treatment (>90%) (Figure 1D). Efficient reduction of ataxin-3 by ASO−/−3 was dose dependent as demonstrated by treatment of control neurons with either 1 or 5 μM ASO−/−3 (Figure S1).

### Screening for allele-specific ASOs targeting the SNP c.987G > C

Based on these results, we selected a treatment duration of 4 days and a concentration of 5 μM for the following experiments to identify an

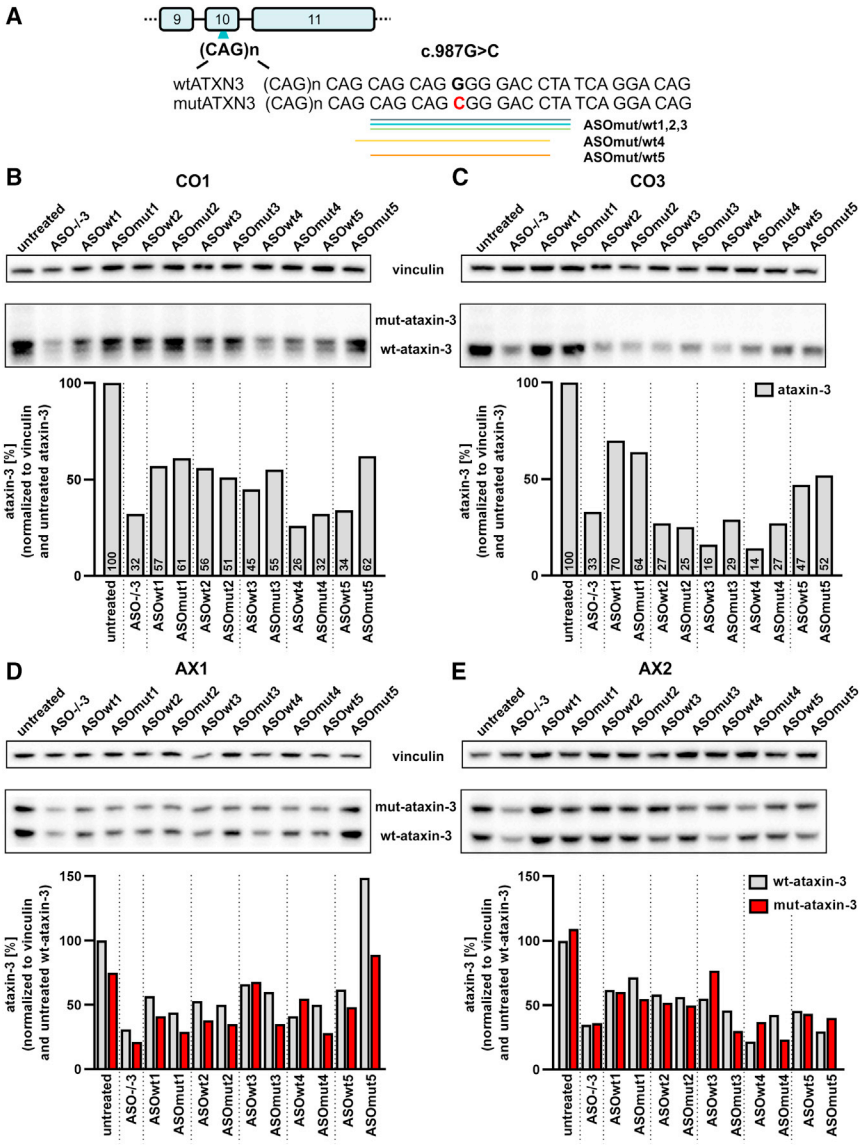


**Figure 2. Screening of potentially allele-specific ASO pairs targeting the SNP c.987G > C**

(A) Scheme and sequence of SNP c.987G > C targeted by allele-specific ASOs ASOmut/wt1 to ASOmut/wt5. (B–E) Ataxin-3 protein expression of untreated, ASO−/−3-treated, and ASOmut/wt1- to ASOmut/wt5-treated iPSC-derived neurons of control lines CO1 (B) and CO3 (C), as well as patient lines AX1 (D) and AX2 (E), analyzed by western blotting. Bands were quantified densitometrically and normalized to vinculin and untreated WT ataxin-3 levels.

ASO that may be able to selectively reduce mutant ataxin-3 in SCA3 iPSC-derived neurons.

We chose SNP c.987G > C as a potential target to achieve allele specificity due to its vicinity to the CAG repeat stretch and its favorable distribution in many European populations. This SNP is frequent in SCA3 alleles and rare in WT alleles, with varying SNP frequencies between European populations. SNP c.987G > C is present in 100% of our Tübingen SCA3 cohort (N = 24) and also present in our three established SCA3 iPSC lines (AX1, AX2, AX3) (Figure S2). We therefore designed five different ASO pairs (ASOmut/wt, Antisense LNA GapmeRs, Qiagen) with different phosphorothioate (PS) backbone modifications and optimized confidential locked nucleic acid (LNA) spike in patterns (Figure 2A). Each pair (ASOmut and ASOwt) differed only at the position of the SNP c.987G > C, while ASOwt was complementary to the WT sequence (G) and ASOmut to the mutant sequence (C) at the desired position.

To analyze the potential of these ASOs to reduce ataxin-3 levels in an allele-specific manner, iPSC-derived neurons of two controls (CO1, CO3) and two patient lines (AX1, AX2) were treated with these 10 different ASOs for 4 days. The already-established allele-unspecific ASO−/−3 was used as a positive control for all experiments. All tested ASOs were able to reduce ataxin-3 protein but with varying efficiencies, as detailed in Figure 2B. Especially, treatment with ASO pair 4 (ASOwt4/ASOmut4) led to a strong reduction in ataxin-3 with an efficiency close to the effect of ASO−/−3. Furthermore, an allele-specific suppression of ataxin-3 could be demonstrated. In control lines, treatment of ASOwt4 led to a stronger reduction of ataxin-3 protein levels compared with treatment with ASOmut4 (Figures 2B and 2C). This effect became even more clearly visible when treating SCA3 iPSC-derived neurons. Since WT and mut-ataxin-3 can easily be discriminated by size in patient cells, an allele-specific effect of ASOs can be visualized by western blot analysis. Treatment of SCA3 neurons with ASOwt4 led to a stronger reduction of WT ataxin-3 compared with mut-ataxin-3, while treatment with ASOmut4 dominantly reduced mut-ataxin-3 compared with WT ataxin-3 levels (Figures 2D and 2E).

### Evaluation of ASOmut4 for selective suppression of poly(Q)-expanded ataxin-3

Based on our screening experiments, we selected ASO pair mut4/wt4 for further studies on kinetics and tolerability of the allele-specific treatment approach.

To further investigate the potential allele-specific effect and the knockdown efficiency of these ASOs, SCA3 iPSC-derived neurons

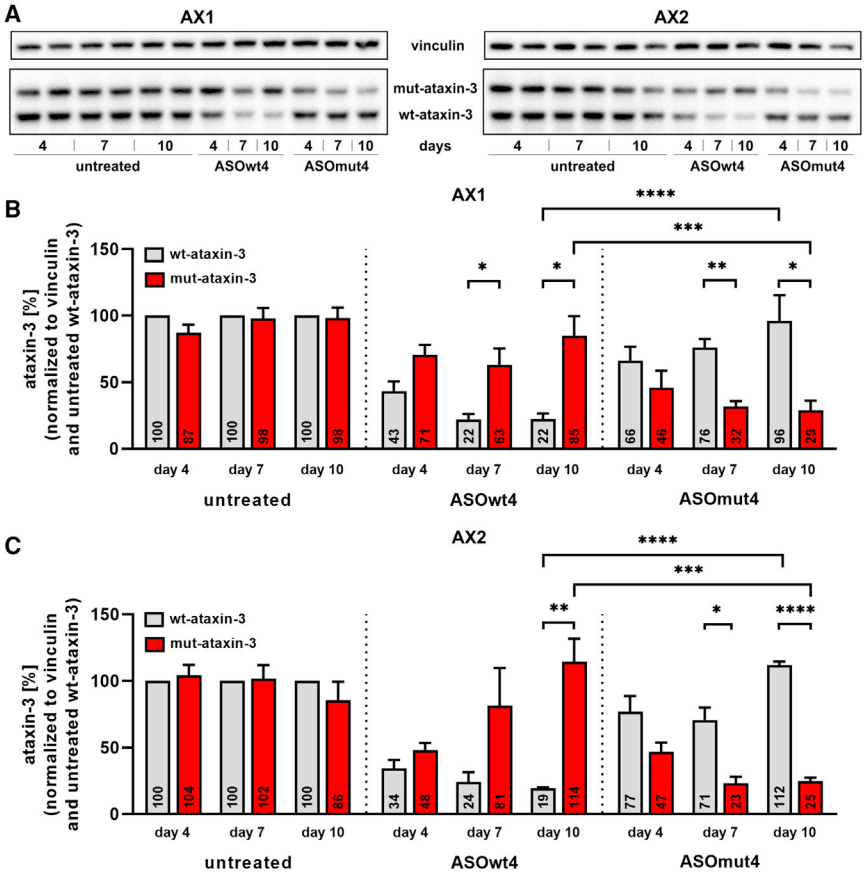


**Figure 3. Time course over 10 days of treatment with allele-specific ASO pair 4**

(A) Ataxin-3 protein expression of untreated, ASOwt4-treated, and ASOmut4-treated iPSC-derived neurons of AX1 (left) and AX2 (right) analyzed by western blotting. One representative blot is shown. (B and C) Bands were quantified densitometrically and normalized to vinculin and untreated WT ataxin-3 levels. Data are the mean ± SEM, n = 3. For statistics of different treatment conditions (ASOwt4 to ASOmut4) at day 10, one-way ANOVA was performed, ***p < 0.001, ****p < 0.0001. For comparison of mut- with WT ataxin-3 levels, unpaired multiple t test was performed, *p < 0.05, **p < 0.01, ****p < 0.0001.

(AX1, AX2) were treated for 4, 7, or 10 days with either ASOwt4 or ASOmut4. Ataxin-3 protein expression was analyzed via western blotting (Figure 3). Statistical analysis revealed again a stable and equal expression of WT and mut-ataxin-3 in untreated samples over time. Treatment of iPSC-derived neurons with ASOwt4 led to a time-dependent reduction in WTATXN3 in both tested SCA3 lines from ∼60% at day 4 to ∼80% at day 10. An initial reduction in mut-ataxin-3 levels of about ∼40% at day 4 returned to baseline levels after 10 days of treatment (Figures 3B and 3C). Comparable effects in the opposite direction could be achieved by treatment with ASOmut4. Protein levels of mut-ataxin-3 decreased by ∼50% at day 4 to ∼75% at day 10, while an initial reduction in WT ataxin-3 (∼30% at day 4) was rescued after 10 days of treatment.

In summary, these results show that a treatment with ASOmut4 in SCA3 iPSC-derived neurons enables an allele-specific targeting of mutATXN3 with an allele-specific knockdown efficiency of ∼75%.

### Long-term efficacy and safety of a single ASO treatment in iPSC-derived neurons

To examine the long-term effect of a single ASO treatment on ataxin-3 levels, iPSC-derived neurons of AX2 were treated for up to 8 weeks (56 days) with ASO−/−3, ASOwt4, or ASOmut4 (Figure 4). Untreated iPSC-derived neurons showed a stable and uniform ataxin-3 expression over time by western blot (Figure 4A). Treatment with ASO−/−3 led to a strong and rather stable reduction in both mutant and WT ataxin-3, with a largely stable efficiency for at least 4 weeks, with ∼95% at day 10 and >90% at day 28. As expected from the previous experiments, treatment with ASOwt4 and ASOmut4 led to diametrical effects on the two alleles (Figure 4B). ASOwt4 treatment reduced the WT ataxin-3 level, being expressed more than 5-fold lower than mut-ataxin-3 at day 10 (ratio of mut-ataxin-3/WT ataxin-3: 5.6) and day 14 (ratio mut-ataxin-3/WT ataxin-3: 5.8) of treatment. On the other hand, ASOmut4 treatment reduced mut-ataxin-3 up to ∼4-fold compared with the WT ataxin-3 level at day 14 (ratio of mut-ataxin-3/WT ataxin-3: 0.28) of treatment (Figure 4C). A gradual recovery of mutant and WT ataxin-3 was observed starting ∼3 weeks after treatment and reaching almost pre-treatment values after 8 weeks.

Results at the protein level could be validated at the RNA level by performing qRT-PCR analysis (Figure 5A). On day 7 of treatment with either ASOwt4 or ASOmut4, *ATXN3* RNA levels were ∼50% reduced (ASOwt4, 0.54; ASOmut4, 0.51), while treatment with ASO−/−3 almost fully erased *ATXN3* RNA at day 7 (ASO−/−3, 0.08). A continuous recovery of *ATXN3* RNA levels could be observed over time, reaching the baseline level at day 28, when treating with either ASOwt4 or ASOmut4, while treatment with ASO−/−3 was still effective at reducing *ATXN3* expression at day 28 (ASO−/−3, 0.60). This observation is in accordance with the previously observed reduction of ataxin-3 protein levels (Figure 4).

To detect potential toxic effects of the ASO treatment on SCA3 iPSC-derived neurons, qRT-PCR of important neuronal cytoskeletal markers (*TUJ*, *MAPT*) as well as lactate dehydrogenase (LDH) cytotoxicity assays were performed. No obvious differences in expression of *TUJ* and *MAPT* could be detected when comparing treated with untreated neurons (Figures 5B and 5C). In addition, no increase in

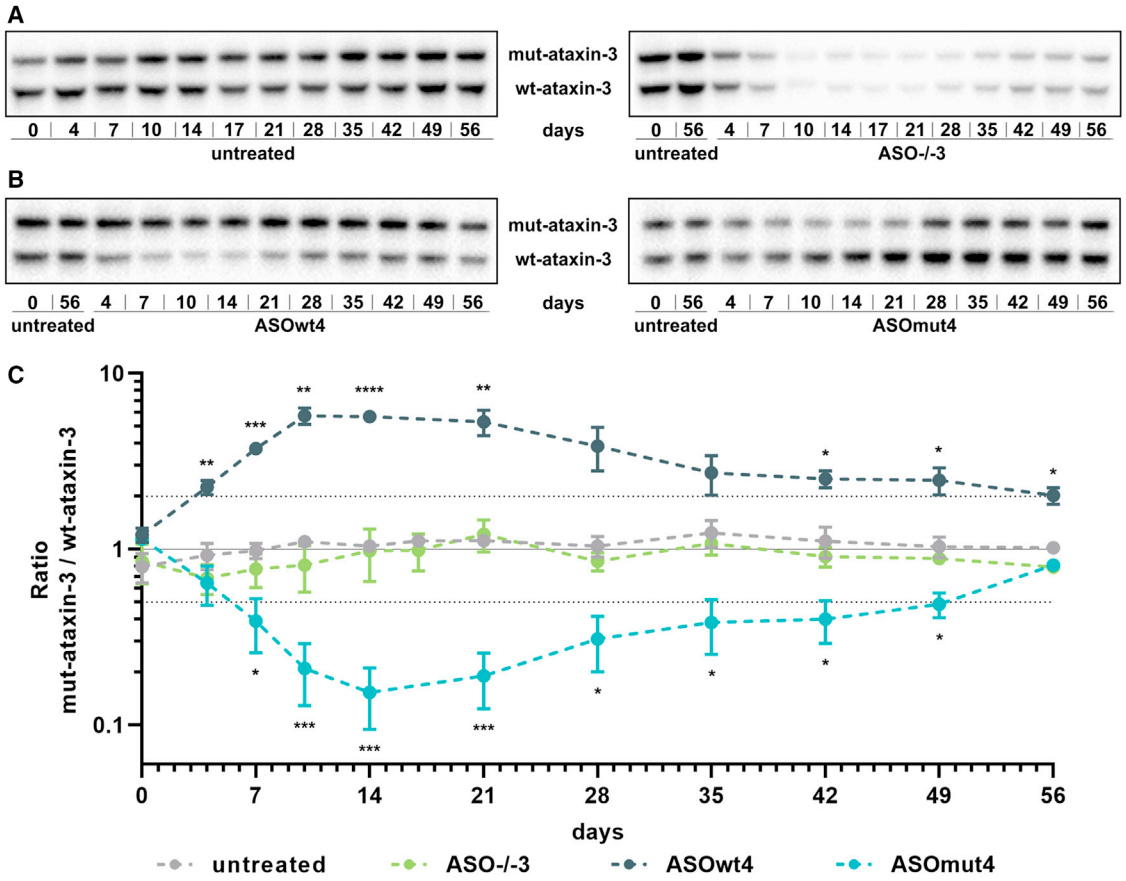


**Figure 4. Long-term treatment over 8 weeks with ASO–/–3 and allele-specific ASOmut/wt4 in iPSC-derived neurons**

(A) Ataxin-3 protein expression of untreated and ASO−/−3-treated iPSC-derived neurons of AX2 analyzed by western blotting. One representative blot is shown. (B) Ataxin-3 protein expression of ASOwt4- and ASOmut4-treated iPSC-derived neurons of patient AX2 analyzed by western blotting. One representative blot is shown. (C) Bands were quantified densitometrically, and the ratio of mut-ataxin-3 to WT ataxin-3 for each day and treatment was determined. Data are the mean ± SEM, n = 3, unpaired multiple t test (untreated to ASO treated), *p < 0.05, **p < 0.01, ***p < 0.001, ****p < 0.0001.

LDH in the supernatant at days 14, 21, and 28 of ASO treatment could be identified in comparison with untreated neurons (Figure 5D). In accordance with this, immunocytochemical staining of SCA3 neurons with TUJ demonstrated no obvious morphological changes upon ASO treatment, with a stable and robust neuronal network present after 14 days of treatment (Figure 5E).

In summary, these results show that a single ASO treatment in SCA3 iPSC-derived neurons is efficient at reducing (mutant) ataxin-3 for several weeks without any obvious sign of neurotoxicity.

## DISCUSSION

The results of our study provide proof of principle that allele-specific lowering of poly(Q)-expanded ataxin-3 by selective ASOs is feasible and long lasting, with sparing of WT ataxin-3 expression, in a human cell culture model that is genetically identical to SCA3 patients.

The generated iPSC-derived neurons provide a platform to screen for therapeutic nucleic acid interventions aiming to lower ataxin-3 expression in SCA3. We believe that human neurons are superior to other *in vitro* models for the analysis of interventions targeting gene expression, as they reflect best the situation in the target organ and are genetically identical to the patient. An efficient knockdown of ataxin-3 could be achieved as early as 4 days of ASO treatment. This makes it possible to screen ASOs within a short period of time. In addition, these ASOs can simply be added to the supernatant and do not need transfection procedures, which highly reduces the complexity of application and leads to a low variability in results between the different cell lines. As small changes in the ASO sequence can have a huge impact on knockdown efficiency, this cellular model can be used to test hundreds of ASOs in a disease-relevant cell type within days. In addition, it allows one to perform toxicity screens by measuring LDH release in the supernatant, as well as pharmacokinetic and dosage studies. We could show that this system has a rather low line-to-line variability and that repeated treatments of single cell lines resulted in very similar effects with minor variability (Figures 2, 3, and 4), proving good reproducibility. In addition, this approach is also feasible for long-term treatments, and analysis over several months is in principle possible.

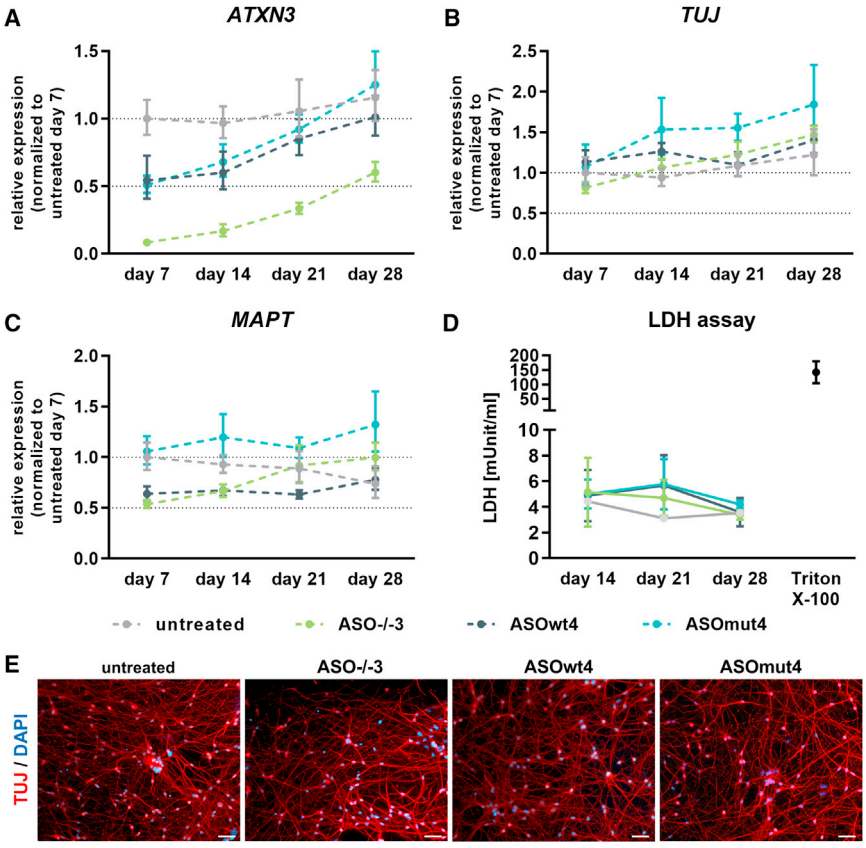


**Figure 5. Gene expression profiling, LDH assay, and immunocytochemical analysis of ASO-treated iPSC-derived neurons of patient AX2**

(A–C) Transcript analysis of *ATXN3* (A), *TUJ* (B), and *MAP2* (C) performed by qRT-PCR at days 7, 14, 21, and 28 of treatment with ASO−/−3, ASOwt4, and ASOmut4. Values are normalized to untreated day 7 and the housekeeping genes *GAPDH* and *TBP*. Data are presented as RQ ± $RQ_{min/max}$, n = 3. (D) LDH release assay at days 14, 21, and 28 of treatment with ASO−/−3, ASOwt4, and ASOmut4. Data are the mean ± SD, n = 3 (E) Immunocytochemical staining of untreated and ASO-treated iPSC-derived neurons for TUJ (green) and DAPI (blue) after 7 days of treatment. Scale bars: 50 μm.

Within this study we prove the efficacy of an ASO approach in SCA3 iPSC-derived neurons leading to a general and stable knockdown of ataxin-3 by ASOs targeting both alleles with an efficiency of >90%. As the ASO approach targets the pre-mRNA of ATXN3, all isoforms are targeted. This should prevent different isoforms in different cell types across the brain from influencing the effectiveness of the ASO treatment. ASOs have already previously been shown to reduce ataxin-3 expression and prevent aggregate formation in SCA3 cellular models and mouse models.[17,18,21] However, these approaches led to a non-selective reduction in both poly(Q)-expanded and WT ataxin-3. As ataxin-3 has several important physiological functions, and as a deubiquitinase is, for example, involved in the proteasomal degradation pathway, it appears desirable to preserve the WT protein as much as possible.

In this study we could show that allele-specific suppression of ataxin-3 is feasible by taking advantage of a SNP in the vicinity of the CAG repeat (SNP c.987G > C). This SNP is present in 100% of our Tübingen SCA3 patient cohort and, in general, in >70% of SCA3 patients.[31] As 14/24 (58.3%) patients of the Tübingen SCA3 cohort are heterozygous for the SNP c.987 with a G on the WT allele, a selective suppression of the mutant allele can be achieved in principle in the majority of SCA3 patients by our approach (Figure S2). Additional SNPs in the ATXN3 gene may be used to apply allele-specific targeting of ASOs for SCA3 patients who are not heterozygous for the SNP c.987. Treatment with an allele-selective ASO designed to target specifically the allele with the expanded CAG stretch (ASOmut4) led to almost 80% reduction in mutant ataxin-3, while the WT level of ataxin-3 remained unchanged after 10 days of treatment. This ASO treatment showed no signs of neurotoxicity as demonstrated by unchanged LDH release up to 4 weeks, no negative effect on *TUJ* and *MAP2* expression up to 4 weeks, and no obvious morphological changes or impaired neuronal networks as analyzed by immunocytochemical staining of TUJ after 14 days of treatment.

A similar approach taking advantage of the SNP c.987 has already been performed in Cos7, HeLa, and 293T cells transfected with expanded and non-expanded ataxin-3 transgenes using siRNAs and shRNAs.[22,40] In these models, different types of short RNA application have been shown to be able to reach allele-selective suppression of the transgenes. Findings in these cell models are in good accordance with our results in SCA3 iPSC-derived neurons, but in an artificial transgene background expressing only the mutant allele and in non-neuronal cells. Alternative approaches aimed at removing the poly(Q) repeat from ataxin-3 by ASO-induced skipping of exon 10.[19] Although this approach helped to reduce aggregates in a SCA3 mouse model, it resulted in a truncated protein with potentially impaired function.

To our knowledge, no SCA3 mouse models are available that fully resemble the human situation with a human WT allele carrying a CAG repeat of normal length and a mutant allele with an expanded CAG repeat. In a rat model that expresses either expanded or WT ataxin-3 after striatal injection of a lentiviral transgene, an allele-specific suppression of the transgene could be reached by lentiviral transfer of shRNAs matching the SNP c.987 with either a C or a G at this position.[22] Whereas this approach proved that the SNP is sufficient to reach some allele-dependent selectivity *in vivo*, it could not explore effects under physiological conditions with simultaneous expression of both alleles. Nevertheless, *in vivo* approaches, e.g., with YAC84Q mice, having a

full-length MJD1 including the SNP c.987G > C,[17] will be the next step to analyze efficiency, tolerability, and safety of the ASOs with favorable performance in human SCA3 neurons, by including functional and pathological readouts. In addition, potential off-target effects of the identified lead ASO need to be validated preferentially *in vivo*. Mouse studies will not be helpful to assess off-target effects, because of the differences between mouse and human genome sequences. Therefore, this analysis needs to be performed in either non-human primates or an advanced human *in vitro* system, like iPSC-derived brain organoids consisting of, ideally, all neural cell types that might be targeted by an intrathecal application prior to an *in vivo* application.

In summary, we conclude that the *in vitro* platform of SCA3 iPSC-derived neurons established in this study is an ideal tool to screen ASOs for efficiency at reducing ataxin-3. We were able to identify a set of ASOs that either exclusively target *ATXN3* in an allele-specific manner or lead to a stable and robust knockdown of ataxin-3 by targeting both alleles. In addition to future functional studies in SCA3 mouse models, these ASOs can be used as *in vitro* tool to investigate the influence of specific knockdown of either WT or poly(Q)-expanded ataxin-3 to further elucidate the pathogenic mechanisms leading to SCA3.

## MATERIALS AND METHODS

### CAG repeat determination

One hundred fifty nanograms of genomic DNA was amplified by a standard PCR followed by capillary electrophoresis using the Beckman Coulter Fragment Analysis Software (Beckman Coulter) and the following primers:

ATXN3_forward, 5′-Cy5-CCAGTGACTACTTTGATTCG-3′;

ATXN3_reverse, 5′-TGGCCTTTCACATGGATGTGAA-3′.

### Determination of SNP c.987G > C

The polymorphism SNP c.987G > C (rs12895357) was determined in an allele-specific manner using two different reverse primers that differ in the base position of SNP c.987 and were each labeled with a different fluorophore, WT sequence G with IRD700 dye and SNP sequence C with Cy5 fluorophore.

One hundred fifty nanograms of genomic DNA was amplified by a standard PCR and analyzed by capillary electrophoresis using the Beckman Coulter Fragment Analysis Software (Beckman Coulter). For PCR amplification the following primers were used:

| Primer | Direction | Sequence (5′-3′) | Fluorophore | Product length (bp) | SNP |
|---|---|---|---|---|---|
| B014 | forward | CCAGTGACT ACTTTGATTCG | – | – | Both |
| G654 | reverse | ACTCTGTCCT GATAGGTCCCC | IRD700 | 181[a] | 987 |
| G655 | reverse | ACTCTGTCCT GATAGGTCCCG | Cy5 | 181[a] | 987 |

[a]Product length depends on CAG repeats; the listed length corresponds to 10 CAG repeats and is the product of the forward and one reverse primer.

### Reprogramming of fibroblasts to iPSCs

Patient and control fibroblasts were reprogrammed by electroporation of $1 \times 10^5$ fibroblasts with 1 μg of episomal plasmids (pCXLE-hUL, pCXLE-hSK, and pCXLE-hOCT4) as described by Okita et al.[41]

In brief, 1 day after electroporation, fibroblast growth factor 2 (FGF-2, 2 ng/mL; Peprotech) was added to Dulbecco's modified Eagle's medium (DMEM), high glucose (Life Technologies), with 10% fetal bovine serum (FBS; Life Technologies). The following day, the cells were cultivated in Essential 8 (E8) medium supplemented with 100 μM sodium butyrate (Sigma-Aldrich) with medium change every other day. Appearing iPSC colonies were manually picked 3–4 weeks after electroporation and further expanded on Matrigel-coated well plates. Splitting and replating of iPSCs were achieved by detachment using PBS/EDTA (0.02% EDTA in PBS). iPSCs were genomically and functionally analyzed according to Hayer et al.[33]

The following lines used in this study:

| Line | Gender | Age at biopsy | *ATXN3* CAG repeat length | *ATXN3* c.987 |
|---|---|---|---|---|
| AX1 | female | 61 years | 23/70 | C/G |
| AX2 | male | 26 years | 26/77 | C/G |
| AX3 | male | 41 years | 24/73 | C/G |
| CO1 | female | 46 years | 14/23 | C/C |
| CO2 | female | 37 years | 23/27 | C/C |
| CO3 | male | 47 years | 21/23 | C/G |

### Differentiation of iPSCs to neurons and ASO treatment

iPSCs were differentiated to neurons of cortical layers V and VI according to published protocols.[38,39,42] In brief, iPSCs were plated in Matrigel-coated plates at a density of $3 \times 10^5$ cells/cm$^2$ in E8 medium supplemented with 10 μM Y-27632 (Selleckchem). Cultivation in 3N medium with 10 μM SB431542 (Sigma-Aldrich) and 500 nM LDN-193189 (Sigma-Aldrich) for 9 days led to neural induction. On day after induction (DAI) 9, the cells were split in a 1:3 ratio and further expanded in 3N medium including 20 ng/mL FGF-2 for 2 days. From DAI 11 to DAI 26, the cells were cultivated in 3N medium with medium change every other day. On DAI 26, the cells were replated at a density of $\sim 7 \times 10^5$ cells/cm$^2$ (protein and RNA isolation) or $1 \times 10^5$ cells/cm$^2$ (immunocytochemistry). The following day, 10 μM PD0325901 (Tocris) and 10 μM DAPT (Sigma Aldrich) were added to 3N medium with an additional medium change at DAI 29. From DAI 31 onward, 3N medium was changed every other day until DAI 36. On DAI 36, ASO treatment was initiated by addition of 5 μM ASO in 200 μL 3N medium to the cells. Two hundred microliters of 3N medium was added to the cells on days 2, 4, 6, and 8. For long-term treatments a full medium change on day 10 (DAI 46) with 3N medium supplemented with 10 ng/mL NGF, BDNF, and GDNF (Peprotech) was performed. Afterward, half-medium changes were conducted three times a week until day 56 (DAI 92).

### ASO design

ASOs used in this study were produced by Qiagen (Antisense LNA GapmeRs) and include PS backbone modifications and an optimized confidential LNA spike in patterns. ASOs were diluted in PBS (stock: 500 μM) and used at a final concentration of 1 or 5 μM.

The following ASOs were used for the initial allele-unspecific ASO screen:

| Description | Sequence |
|---|---|
| ASO−/−1 | ATCTTCGTCTAACATT |
| ASO−/−2 | CGTAGGGCTTAAAACG |
| ASO−/−3 | TAGTAACTCCTCCTTC |
| ASO−/−4 | AAAACTGATTGGCACA |
| ASO−/−5 | AAACCGCTAAAAGTCT |

The following ASOs were designed and tested for allele-specific targeting of the SNP c.987G > C.

| Description | Sequence (ASOmut) | Sequence (ASOwt) |
|---|---|---|
| ASOmut/wt1 | TAGGTCCCGCTGCTG | TAGGTCCCCCTGCTG |
| ASOmut/wt2 | TAGGTCCCGCTGCTG | TAGGTCCCCCTGCTG |
| ASOmut/wt3 | TAGGTCCCGCTGCTG | TAGGTCCCCCTGCTG |
| ASOmut/wt4 | GGTCCCGCTGCTGC | GGTCCCCCTGCTGC |
| ASOmut/wt5 | GGTCCCGCTGCTG | GGTCCCCCTGCTG |

### Western blotting

Pellets of iPSC-derived neurons were lysed in RIPA buffer (Sigma-Aldrich) supplemented with 1× cOmplete protease inhibitor cocktail (PI) (Roche) for 45 min on a rotator at 4°C. Cell debris was pelleted at 15,800*g* at 4°C for 30 min, and the supernatant protein content was analyzed. Protein concentration was determined using the Pierce BCA Protein Assay Kit (Thermo Fisher Scientific) according to the manufacturer's guidelines.

Five micrograms of protein was eluted in 5× Buffer Pink (Thermo Fisher Scientific) and heated to 95°C. Samples were loaded and separated on 10% polyacrylamide gels in 1× NuPAGE MOPS SDS running buffer (Novex). Proteins were transferred onto a Hybond-P polyvinylidene difluoride membrane (Merck Millipore) at 4°C overnight. Blocking was performed in 5% skimmed milk in TBS-T. Primary antibodies were diluted in Western Blocking Reagent (Roche) and incubated overnight at 4°C. The following antibodies were used: anti-vinculin (V9131, mouse, 1:100,000; Merck) and anti-ataxin-3 (13H9L9, rabbit, 1:5,000; Thermo Fisher Scientific). After three washes with TBS-T, incubation with HRP-conjugated secondary antibodies (Jackson ImmunoResearch) for 1 h at room temperature was performed. Proteins were visualized using the Immobilon western chemiluminescent HRP substrate (Merck Millipore) and the imager ChemiDoc MP (Bio-Rad). Bands were quantified with ImageJ and normalized to their respective loading controls.

### qRT-PCR

RNA isolation of iPSC-derived neurons at days 7, 14, 21, and 28 of ASO treatment was performed using the RNeasy Mini Kit (Qiagen) according to the manufacturer's instructions. Two hundred fifty nanograms of isolated RNA of each sample was reverse transcribed to cDNA by using the RevertAid First Strand cDNA Synthesis Kit (Thermo Fisher Scientific) according to the manufacturer's guidelines. Quantitative real-time PCR was performed on a ViiA 7 Real-Time PCR System (Applied Biosystems) in triplicate per sample by adding 3 μL cDNA (1.25 ng/μL) to 2 μL primer pairs (2 μM) and 5 μL SYBR Green Select Master Mix (Applied Biosystems). GAPDH and TBP were used as housekeeping genes and relative quantification (RQ) values ($RQ_{min}/RQ_{max}$) were determined.

For amplification the following primers were used:

| Primer | Forward sequence (5′-3′) | Reverse sequence (5′-3′) |
|---|---|---|
| GAPDH | TCACCAGGGCTG CTTTTAAC | GACAAGCTTCCCGTTCTCAG |
| TBP | CTTCGGAGAGTTC TGGGATTG | CACGAAGTGCAATGGTCTTTAG |
| ATXN3 | GATCTAGGTGATGCT ATGAGTG | GTGGACCCTATGCTGTAATC |
| TUJ | GCAACTACGTGGGCGACT | GGCCTGAAGAGATGTCCAAA |
| MAP2 | CCCTGGCGGAGGA AATAAAA | TCTTGGCTTTGGCGTTCTC |

The following qRT-PCR program was used: 50°C for 2 min; 95°C for 2 min; followed by 40 cycles of 95°C for 1 s, 60°C for 30 s, and 72°C for 5 s; and subsequently 95°C for 15 s, 60°C for 1 min, and 95°C for 15 s. The specificity of PCR products was confirmed by melting curve analysis. Analysis was performed with QuantStudio Software v.1.3 (Thermo Fisher Scientific).

### LDH assay

For the quantification of LDH in the supernatant of cultivated iPSC-derived neurons, the LDH-Glo Cytotoxicity Assay (Promega) was used according to the manufacturer's instructions. In brief, 10 μL supernatant was collected 14, 21, and 28 days after ASO treatment and diluted in 190 μL LDH storage buffer. Assay was performed in triplicate per sample according to the manufacturer's guidelines and analyzed after 1 h incubation using a Spectramax M2e plate reader (Molecular Devices).

### Immunocytochemistry

iPSC-derived neurons were fixed on DAI 50 (ASO treatment day 14) with 4% paraformaldehyde (PFA; Merck Millipore) for 15 min and subsequently washed with PBS. After blocking and permeabilization using 5% BSA (Sigma Aldrich) and 0.1% Triton X-100 (Carl Roth) in PBS, iPSC-derived neurons were stained with anti-β-III-tubulin (TUJ, mouse, 1:1,000, T8660; Sigma Aldrich). After an additional washing step, Alexa Fluor-conjugated secondary antibody (Thermo Fisher Scientific) was applied. Nuclei were stained with Hoechst

33258 (1:10,000, H1398, Thermo Fisher Scientific). Coverslips were mounted with EverBrite mounting medium (Biotium) and images acquired using a Zeiss Observer Z1 fluorescence microscope (Carl Zeiss).

## SUPPLEMENTAL INFORMATION

Supplemental information can be found online at https://doi.org/10.1016/j.omtn.2021.11.015.

## ACKNOWLEDGMENTS

We thank the patients and their families for their contributions. We would like to thank Isabelle Meyer, Elene Dal Ferro, Rainer Kuhn, Mark Gemkow, Christoph Wiessner, and Bastian Zimmer (Evotec SE, Hamburg, Germany) for their support. The work of L.S. has been supported by the Germany Ministry of Education and Research (BMBF grant 01ED16028). Figure 1A was created with BioRender.com. We acknowledge support by the Open Access Publishing Fund of the University of Tuebingen.

## AUTHOR CONTRIBUTIONS

Conceptualization, S.H. and L.S.; methodology, S.H.; formal analysis, S.H. and J.H.; investigation, S.H., J.H., M. Kraft, M. Korneck, and J. H.-S.; resources, J. H.-S.; writing – original draft, S.H. and L.S.; writing – review & editing, J.H., M. Kraft, M. Korneck, and J. H.-S.; visualization, S.H. and J.H.; supervision, S.H. and L.S.; project administration, S.H. and L.S.; funding acquisition, L.S.

## DECLARATION OF INTERESTS

The authors declare no competing interests.

## REFERENCES

1. Kawaguchi, Y., Okamoto, T., Taniwaki, M., Aizawa, M., Inoue, M., Katayama, S., Kawakami, H., Nakamura, S., Nishimura, M., Akiguchi, I., et al. (1994). CAG expansions in a novel gene for Machado-Joseph disease at chromosome 14q32.1. Nat. Genet. *8*, 221–228.
2. Matos, C.A., de Almeida, L.P., and Nóbrega, C. (2019). Machado–Joseph disease/spinocerebellar ataxia type 3: lessons from disease pathogenesis and clues into therapy. J. Neurochem. *148*, 8–28.
3. Chai, Y., Koppenhafer, S.L., Shoesmith, S.J., Perez, M.K., and Paulson, H.L. (1999). Evidence for proteasome involvement in polyglutamine disease: localization to nuclear inclusions in SCA3/MJD and suppression of polyglutamine aggregation in vitro. Hum. Mol. Genet. *8*, 673–682.
4. Seidel, K., den Dunnen, W.F., Schultz, C., Paulson, H., Frank, S., de Vos, R.A., Brunt, E.R., Deller, T., Kampinga, H.H., and Rüb, U. (2010). Axonal inclusions in spinocerebellar ataxia type 3. Acta Neuropathol. *120*, 449–460.
5. Schmidt, T., Landwehrmeyer, G.B., Schmitt, I., Trottier, Y., Auburger, G., Laccone, F., Klockgether, T., Völpel, M., Epplen, J.T., and Schöls, L. (1998). An isoform of ataxin-3 accumulates in the nucleus of neuronal cells in affected brain regions of SCA3 patients. Brain Pathol. *8*, 669–679.
6. Takahashi, J., Tanaka, J., Arai, K., Funata, N., Hattori, T., Fukuda, T., Fujigasaki, H., and Uchihara, T. (2001). Recruitment of nonexpanded polyglutamine proteins to intranuclear aggregates in neuronal intranuclear hyaline inclusion disease. J. Neuropathol. Exp. Neurol. *60*, 369–376.
7. Seidel, K., Siswanto, S., Fredrich, M., Bouzrou, M., Brunt, E., van Leeuwen, F., Kampinga, H., Korf, H.W., Rüb, U., and den Dunnen, W. (2016). Polyglutamine aggregation in H untington's disease and spinocerebellar ataxia type 3: similar mechanisms in aggregate formation. Neuropathol. Appl. Neurobiol. *42*, 153–166.
8. Matsumoto, M., Yada, M., Hatakeyama, S., Ishimoto, H., Tanimura, T., Tsuji, S., Kakizuka, A., Kitagawa, M., and Nakayama, K.I. (2004). Molecular clearance of ataxin-3 is regulated by a mammalian E4. EMBO J. *23*, 659–669.
9. Durcan, T.M., Kontogiannea, M., Thorarinsdottir, T., Fallon, L., Williams, A.J., Djarmati, A., Fantaneanu, T., Paulson, H.L., and Fon, E.A. (2011). The Machado–Joseph disease-associated mutant form of ataxin-3 regulates parkin ubiquitination and stability. Hum. Mol. Genet. *20*, 141–154.
10. Ashkenazi, A., Bento, C.F., Ricketts, T., Vicinanza, M., Siddiqi, F., Pavel, M., Squitieri, F., Hardenberg, M.C., Imarisio, S., and Menzies, F.M. (2017). Polyglutamine tracts regulate beclin 1-dependent autophagy. Nature *545*, 108–111.
11. Herzog, L.K., Kevei, É., Marchante, R., Böttcher, C., Bindesbøll, C., Lystad, A.H., Pfeiffer, A., Gierisch, M.E., Salomons, F.A., and Simonsen, A. (2020). The Machado–Joseph disease deubiquitylase ataxin-3 interacts with LC3C/GABARAP and promotes autophagy. Aging Cell *19*, e13051.
12. Chen, X., Tang, T.-S., Tu, H., Nelson, O., Pook, M., Hammer, R., Nukina, N., and Bezprozvanny, I. (2008). Deranged calcium signaling and neurodegeneration in spinocerebellar ataxia type 3. J. Neurosci. *28*, 12713–12724.
13. Chou, A.-H., Yeh, T.-H., Ouyang, P., Chen, Y.-L., Chen, S.-Y., and Wang, H.-L. (2008). Polyglutamine-expanded ataxin-3 causes cerebellar dysfunction of SCA3 transgenic mice by inducing transcriptional dysregulation. Neurobiol. Dis. *31*, 89–101.
14. Li, F., Macfarlan, T., Pittman, R.N., and Chakravarti, D. (2002). Ataxin-3 is a histone-binding protein with two independent transcriptional corepressor activities. J. Biol. Chem. *277*, 45004–45012.
15. Chou, A.-H., Yeh, T.-H., Kuo, Y.-L., Kao, Y.-C., Jou, M.-J., Hsu, C.-Y., Tsai, S.-R., Kakizuka, A., and Wang, H.-L. (2006). Polyglutamine-expanded ataxin-3 activates mitochondrial apoptotic pathway by upregulating Bax and downregulating Bcl-xL. Neurobiol. Dis. *21*, 333–345.
16. Harmuth, T., Prell-Schicker, C., Weber, J.J., Gellerich, F., Funke, C., Drießen, S., Magg, J.C., Krebiehl, G., Wolburg, H., and Hayer, S.N. (2018). Mitochondrial morphology, function and homeostasis are impaired by expression of an N-terminal calpain cleavage fragment of ataxin-3. Front. Mol. Neurosci. *11*, 368.
17. McLoughlin, H.S., Moore, L.R., Chopra, R., Komlo, R., McKenzie, M., Blumenstein, K.G., Zhao, H., Kordasiewicz, H.B., Shakkottai, V.G., and Paulson, H.L. (2018). Oligonucleotide therapy mitigates disease in spinocerebellar ataxia type 3 mice. Ann. Neurol. *84*, 64–77.
18. Moore, L.R., Rajpal, G., Dillingham, I.T., Qutob, M., Blumenstein, K.G., Gattis, D., Hung, G., Kordasiewicz, H.B., Paulson, H.L., and McLoughlin, H.S. (2017). Evaluation of antisense oligonucleotides targeting ATXN3 in SCA3 mouse models. Mol. Ther. Nucleic Acids *7*, 200–210.
19. Toonen, L.J., Rigo, F., van Attikum, H., and van Roon-Mom, W.M. (2017). Antisense oligonucleotide-mediated removal of the polyglutamine repeat in spinocerebellar ataxia type 3 mice. Mol. Ther. Nucleic Acids *8*, 232–242.
20. Nobrega, C., Codesso, J.M., Mendonca, L., and Pereira de Almeida, L. (2019). RNA interference therapy for Machado–Joseph disease: long-term safety profile of lentiviral vectors encoding short hairpin RNAs targeting mutant ataxin-3. Hum. Gene Ther. *30*, 841–854.
21. Moore, L.R., Keller, L., Bushart, D.D., Delatorre, R.G., Li, D., McLoughlin, H.S., do Carmo Costa, M., Shakkottai, V.G., Smith, G.D., and Paulson, H.L. (2019). Antisense oligonucleotide therapy rescues aggresome formation in a novel spinocerebellar ataxia type 3 human embryonic stem cell line. Stem Cell Res. *39*, 101504.
22. Alves, S., Nascimento-Ferreira, I., Auregan, G., Hassig, R., Dufour, N., Brouillet, E., de Lima, M.C.P., Hantraye, P., de Almeida, L.P., and Déglon, N. (2008). Allele-specific RNA silencing of mutant ataxin-3 mediates neuroprotection in a rat model of Machado-Joseph disease. PLoS One *3*, e3341.
23. Li, Y., Yokota, T., Matsumura, R., Taira, K., and Mizusawa, H. (2004). Sequence-dependent and independent inhibition specific for mutant ataxin-3 by small interfering RNA. Ann. Neurol. *56*, 124–129.
24. Nóbrega, C., Nascimento-Ferreira, I., Onofre, I., Albuquerque, D., Hirai, H., Déglon, N., and de Almeida, L.P. (2013). Silencing mutant ataxin-3 rescues motor deficits and neuropathology in Machado-Joseph disease transgenic mice. PLoS One *8*, e52396.
25. Conceição, M., Mendonça, L., Nóbrega, C., Gomes, C., Costa, P., Hirai, H., Moreira, J.N., Lima, M.C., Manjunath, N., and de Almeida, L.P. (2016). Intravenous

administration of brain-targeted stable nucleic acid lipid particles alleviates Machado-Joseph disease neurological phenotype. Biomaterials *82*, 124–137.

26. Rodríguez-Lebrón, E., doCarmo Costa, M., Luna-Cancalon, K., Peron, T.M., Fischer, S., Boudreau, R.L., Davidson, B.L., and Paulson, H.L. (2013). Silencing mutant ATXN3 expression resolves molecular phenotypes in SCA3 transgenic mice. Mol. Ther. *21*, 1909–1918.

27. Carmona, V., Cunha-Santos, J., Onofre, I., Simões, A.T., Vijayakumar, U., Davidson, B.L., and de Almeida, L.P. (2017). Unravelling endogenous microRNA system dysfunction as a new pathophysiological mechanism in Machado-Joseph disease. Mol. Ther. *25*, 1038–1055.

28. Evers, M.M., Tran, H.-D., Zalachoras, I., Pepers, B.A., Meijer, O.C., den Dunnen, J.T., van Ommen, G.-J.B., Aartsma-Rus, A., and van Roon-Mom, W.M. (2013). Ataxin-3 protein modification as a treatment strategy for spinocerebellar ataxia type 3: removal of the CAG containing exon. Neurobiol. Dis. *58*, 49–56.

29. Kourkouta, E., Weij, R., González-Barriga, A., Mulder, M., Verheul, R., Bosgra, S., Groenendaal, B., Puoliväli, J., Toivanen, J., and van Deutekom, J.C. (2019). Suppression of mutant protein expression in SCA3 and SCA1 mice using a CAG repeat-targeting antisense oligonucleotide. Mol. Ther. Nucleic Acids *17*, 601–614.

30. Maciel, P., Gaspar, C., Guimaraes, L., Goto, J., Lopes-Cendes, I., Hayes, S., Arvidsson, K., Dias, A., Sequeiros, J., and Sousa, A. (1999). Study of three intragenic polymorphisms in the Machado-Joseph disease gene (MJD1) in relation to genetic instability of the (CAG) n tract. Eur. J. Hum. Genet. *7*, 147–156.

31. Gaspar, C., Lopes-Cendes, I., Hayes, S., Goto, J., Arvidsson, K., Dias, A., Silveira, I., Maciel, P., Coutinho, P., and Lima, M. (2001). Ancestral origins of the Machado-Joseph disease mutation: a worldwide haplotype study. Am. J. Hum. Genet. *68*, 523–528.

32. Takahashi, K., and Yamanaka, S. (2006). Induction of pluripotent stem cells from mouse embryonic and adult fibroblast cultures by defined factors. Cell *126*, 663–676.

33. Hayer, S.N., Schelling, Y., Huebener-Schmid, J., Weber, J.J., Hauser, S., and Schöls, L. (2018). Generation of an induced pluripotent stem cell line from a patient with spinocerebellar ataxia type 3 (SCA3): HIHCNi002-A. Stem Cell Res. *30*, 171–174.

34. Ou, Z., Luo, M., Niu, X., Chen, Y., Xie, Y., He, W., Song, B., Xian, Y., Fan, D., and OuYang, S. (2016). Autophagy promoted the degradation of mutant ATXN3 in neurally differentiated spinocerebellar ataxia-3 human induced pluripotent stem cells. Biomed. Res. Int. *2016*, 6701793.

35. Chuang, C.-Y., Yang, C.-C., Soong, B.-W., Yu, C.-Y., Chen, S.-H., Huang, H.-P., and Kuo, H.-C. (2019). Modeling spinocerebellar ataxias 2 and 3 with iPSCs reveals a role for glutamate in disease pathology. Sci. Rep. *9*, 1–13.

36. Koch, P., Breuer, P., Peitz, M., Jungverdorben, J., Kesavan, J., Poppe, D., Doerr, J., Ladewig, J., Mertens, J., and Tüting, T. (2011). Excitation-induced ataxin-3 aggregation in neurons from patients with Machado–Joseph disease. Nature *480*, 543–546.

37. Hansen, S.K., Stummann, T.C., Borland, H., Hasholt, L.F., Tümer, Z., Nielsen, J.E., Rasmussen, M.A., Nielsen, T.T., Daechsel, J.C., and Fog, K. (2016). Induced pluripotent stem cell-derived neurons for the study of spinocerebellar ataxia type 3. Stem Cell Res. *17*, 306–317.

38. Schuster, S., Heuten, E., Velic, A., Admard, J., Synofzik, M., Ossowski, S., Macek, B., Hauser, S., and Schöls, L. (2020). CHIP mutations affect the heat shock response differently in human fibroblasts and iPSC-derived neurons. Dis. Model. Mech. *13*, dmm045096.

39. Hauser, S., Schuster, S., Heuten, E., Höflinger, P., Admard, J., Schelling, Y., Velic, A., Macek, B., Ossowski, S., and Schöls, L. (2020). Comparative transcriptional profiling of motor neuron disorder-associated genes in various human cell culture models. Front. Cell Dev. Biol. *8*, 544043.

40. Miller, V.M., Xia, H., Marrs, G.L., Gouvion, C.M., Lee, G., Davidson, B.L., and Paulson, H.L. (2003). Allele-specific silencing of dominant disease genes. Proc. Natl. Acad. Sci. U S A *100*, 7195–7200.

41. Okita, K., Matsumura, Y., Sato, Y., Okada, A., Morizane, A., Okamoto, S., Hong, H., Nakagawa, M., Tanabe, K., Tezuka, K., et al. (2011). A more efficient method to generate integration-free human iPS cells. Nat. Methods *8*, 409–412.

42. Rehbach, K., Kesavan, J., Hauser, S., Ritzenhofen, S., Jungverdorben, J., Schüle, R., Schöls, L., Peitz, M., and Brüstle, O. (2019). Multiparametric rapid screening of neuronal process pathology for drug target identification in HSP patient-specific neurons. Sci. Rep. *9*, 1–13.